Multi-element, high-temperature integrated ultrasonic transducers for structural health monitoring

Veilleux, Jocelyn; Kruger, Silvio E.; Wu, Kuo-ting; Blouin, Alain

Publisher's version / Version de l'éditeur:
https://doi.org/10.1117/12.2009868
SPIE Smart Structures and Materials + Nondestructive Evaluation and Health Monitoring, pp. 86930I-1-86930I-8, 2013-02-01

Multi-element, high-temperature integrated ultrasonic transducers for structural health monitoring

Jocelyn Veilleux*, Silvio E. Kruger, Kuo-Ting Wu and Alain Blouin#
National Research Council Canada, 75 de Mortagne Blvd., Boucherville, QC, Canada, J4B 6Y4

ABSTRACT

This paper reports recent developments on high-temperature, multi-element integrated ultrasonic transducers (IUTs). The multi-element IUTs are fabricated from a sol-gel route, where piezoelectric films are deposited, poled and machined into an array of 16 elements. Electrical wiring and insulation are also integrated into a practical, simple high-temperature assembly. These multi-element IUTs show a high potential for structural health monitoring at high temperatures (in the 200-500°C range): they can withstand thermal cycling and shocks, they can be integrated to complex geometries, and they have broadband and suitable operating frequency characteristics with a minimal footprint (no backing needed). The specifics of multi-element transducers, including the phased array approach, for structural health monitoring are discussed.

Keywords: ultrasonic transducer, phased array, PZT, sol-gel, high temperature

1. INTRODUCTION

Replacing schedule-based maintenance with condition-based maintenance is an important objective of structural health monitoring (SHM). To improve the cost-effectiveness of SHM, damages that adversely affect the structure must be detected at an early stage (i.e. sufficient sensitivity under operating conditions), and the monitoring hardware must be affordable to allow its permanent integration to the structure. In several cases, especially in the aerospace, power and oil and gas industries, the sensor network must be easily deployable on existing structures, either under operating conditions or during a brief downtime/shutdown[1-3]. If it is well established that piezoelectric ultrasonic transducers (UTs) are widely used for real-time nondestructive testing (NDT) and evaluation of large structures[4], including airplanes, steam pipes, and pipelines, their large-scale integration to complex structures and deployment in high-temperature environments still require research and development. Indeed, common limitations of piezoelectric UTs shall be addressed to ensure effective SHM in such conditions[5]:

a. A couplant is necessary to transmit ultrasounds;
b. A backing material is required;
c. The usage of UTs above 60°C is difficult;
d. The conformal mapping of UTs to curved geometries is problematic.

It has been shown that most of these limitations can be overcome with sol-gel sprayed lead-zirconate-titanate (PZT)/PZT composite UT films, often referred to as high-temperature integrated ultrasonic transducers (IUTs)[5-8]. When used in pulse-echo mode for example, they are effective in monitoring pipe wall thickness at temperatures up to 200°C for PZT/PZT IUTs and up to 500°C for bismuth titanate (BIT)/PZT IUTs[8]. In an effort to further improve the technology of sol-gel sprayed composite UT films and to expand their range of NDT applications to methods requiring beam focusing and aiming, this paper reports recent development on multi-element high-temperature integrated ultrasonic transducers (IUTs). The multi-element IUTs are fabricated from a sol-gel route, where the piezoelectric films are deposited, poled and machined into an array of 16 elements. It is shown that both PZT/PZT and BIT/PZT IUTs were successfully machined into arrays of 16 elements, that the center frequency and bandwidth of each element of a given array have small variances, and that the acoustic field generated by a given element is relatively uniform.

* Current position: Assistant Professor, Department of Chemical Engineering and Biotechnological Engineering, Université de Sherbrooke, 2500 Université Blvd., Sherbrooke, QC, Canada, J1K 2R1
# alain.blouin@cnrc-nrc.gc.ca; tel.: (450) 641-5112; fax: (450) 641-5106 http://www.nrc-cnrc.gc.ca

2. FABRICATION OF THE MULTI-ELEMENT IUTS

2.1 Sol-gel route

Thick composite piezoelectric films (tens of μm) were fabricated from a sol-gel route, as proposed by Barrow *et al.*[9], for which a process flow chart is shown in Figure 1. A piezoelectric powder (PZT and BIT were chosen in the present study) is dispersed into PZT sol-gel precursors by ball milling and the mixture is air-sprayed onto a substrate (a titanium alloy was chosen hereafter). Then, heat treatments are applied to cure the deposited layer and the process is repeated until the desired thickness is obtained. Single layer thickness is dictated by process concerns, whereas the final film thickness (several layers) is related to the center frequency response of the UT. The film obtained was electrically poled by means of a corona discharge and a silver top electrode was deposited by PVD. The bottom electrode was the substrate itself. This process resulted in a single element IUT, directly bonded to the titanium alloy, where the cured PZT sol-gel bonds the piezoelectric powder grains together and to the substrate. Such a composite piezoelectric film has a porous microstructure that withstands thermal cycling and thermal shocks. When deposited onto a thin, flexible substrate, the resulting IUT is also flexible[10].

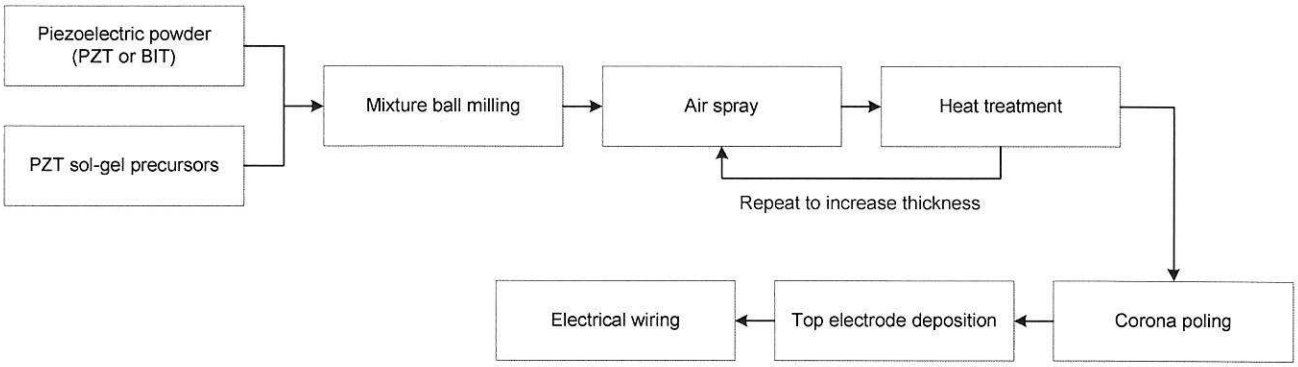

Figure 1. Process flow chart for the fabrication of a composite piezoelectric UT film, from a sol-gel route.

2.2 Designing and machining multi-element IUTs

The next step consisted in designing the multi-element IUTs and in machining the single-element IUT into an array of 16 elements, as shown in Figure 2. The width, gap and pitch of the multi-element IUTs were determined using conventional design rules for phased arrays[11-12], that is width $e < \lambda/2$, pitch $p < 0.67\lambda$ and gap $g = p - e$. Knowing that steel and titanium alloys are likely substrates for multi-element IUTs applications, the longitudinal ultrasonic wave velocity $c \sim 5.6 - 6.2$ mm/μs leads to a wavelength $\lambda \sim 1 - 2$ mm for a frequency $f \sim 3 - 6$ MHz. It follows that the element width $e \sim 500$ μm, pitch $p \sim 700$ μm and gap $g \sim 200$ μm.

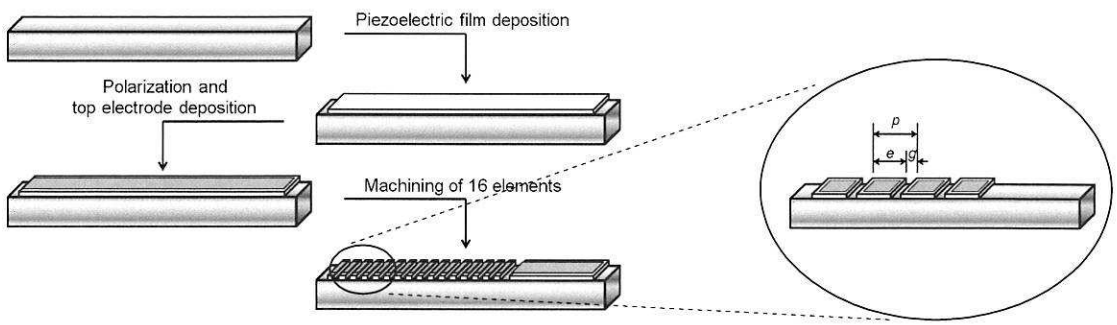

Figure 2. Process flow chart for the fabrication of multi-element IUTs. The insert shows a schematic representation of the element width (e), gap (g) and pitch (p) on the multi-element IUT.

Such dimensions (hundreds of μm) are compatible with mechanical machining using a slit cutter, which was the means chosen to cut into the deposited thick piezoelectric PZT/PZT and BIT/PZT films. Optical micrographs of the machined are shown in Figure 3. The 16 elements' width and gap regularity can be appreciated in both cases, but the slit sharpness seems better in the case of PZT/PZT. It is suggested that the BIT/PZT films are more brittle, which lead to the observed chipping behavior near the edges of the elements.

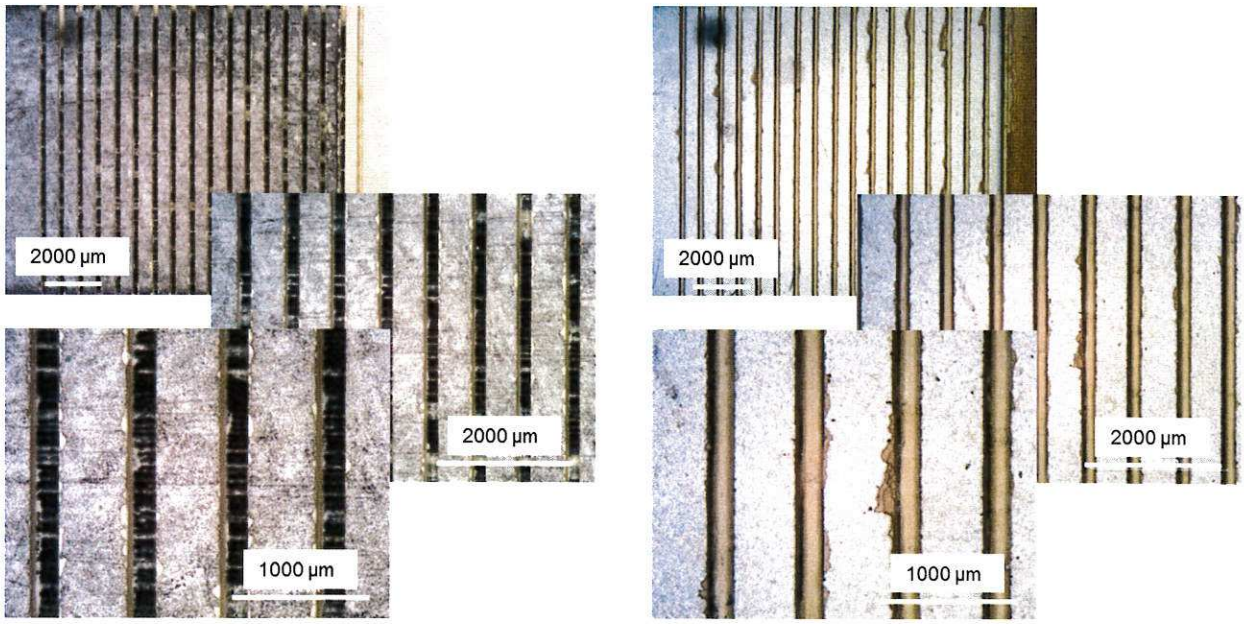

Figure 3. Optical micrographs of the fabricated multi-element PZT/PZT (left) and BIT/PZT (right) IUTs. The elements widths and gaps are uniform, although some of the BIT/PZT elements were damaged when being machined.

3. TIME SIGNALS OF THE MULTI-ELEMENT IUTS

The 16 elements of the PZT/PZT and BIT/PZT multi-element IUTs were individually excited in pulse-echo mode to test their uniformity along the array. A Panametrics 5072PR pulser-receiver with broadband negative spike excitation was used to drive the IUTs. Examples of time signals and first echoes frequency spectra for the 16 elements are shown in Figure 4 for PZT/PZT and in Figure 5 for BIT/PZT. The superimposed time signals show that the first and second echoes have a quasi-constant phase among the 16 elements, which illustrates that the porous microstructure of the deposited films is sufficiently uniform at the macroscopic scale to avoid microstructure-induced propagation delays.

Oppositely, the measured amplitudes for the first echoes vary by a factor 2 between the strongest and weakest elements (better appreciated in Figures 6-7). The quality of the electrical contacts, either between the wire and the top electrode or within the top electrode itself, is likely responsible for this observed behavior. Indeed, the thin PVD deposited silver top electrodes may have regions of lower or zero electrical conduction, due to surface roughness or damages induced by manipulation of the arrays for example. Chipped element edges in the BIT/PZT film can also adversely affect the magnitude of the signal. In should be noted here that the receiver gain used for the PZT/PZT and BIT/PZT elements was +20 dB and +34 dB, respectively. This difference is expected, as the d_{33} value is much greater for PZT than for BIT.

The first echo center frequency and -6 dB bandwidth of each element are compared in Figures 6-7. Both are quite stable at 3.2 MHz and 35% for the PZT/PZT film, whereas the bimodal frequency spectrum makes it harder to interpret for the BIT/PZT film. An average of 6.5 MHz was found by the simple algorithm used (identification of a maximum on the frequency spectrum), but a value of 5.5 MHz is more realistic if one makes abstraction of the bimodal distribution. The latter could be the result of destructive interference at this frequency, an artifact likely introduced by the film thickness. The -6 dB bandwidth is broader, at 50-60%.

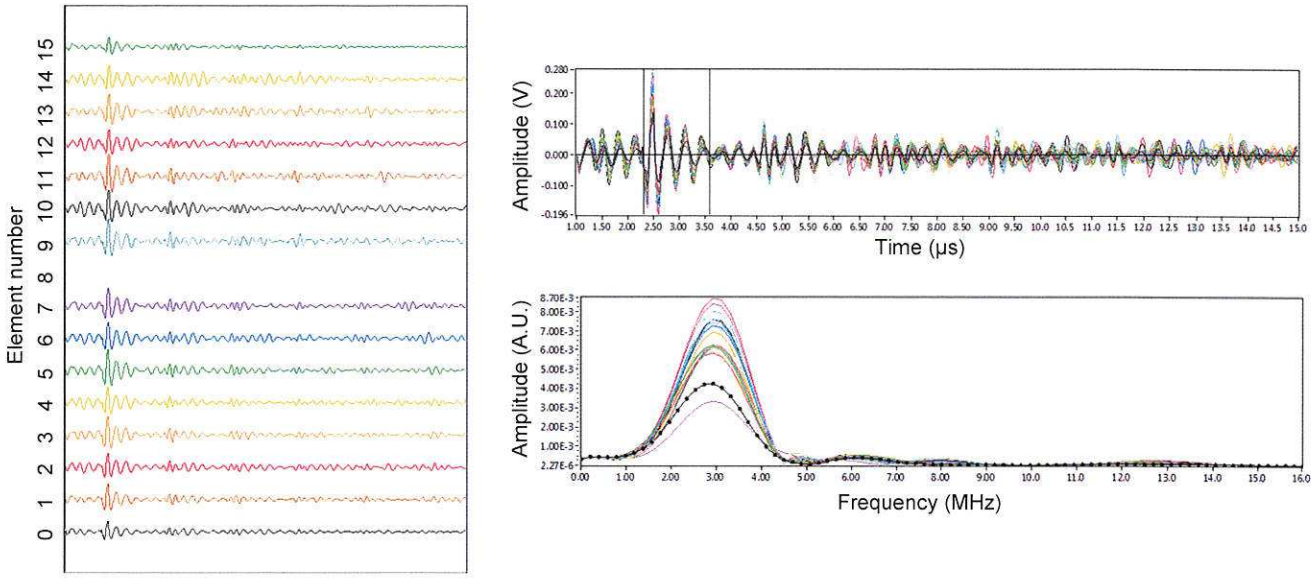

Figure 4. PZT/PZT elements time signals (pulse-echo). Top right: superimposed time signals. Bottom right: frequency spectrum of the first echo for each element.

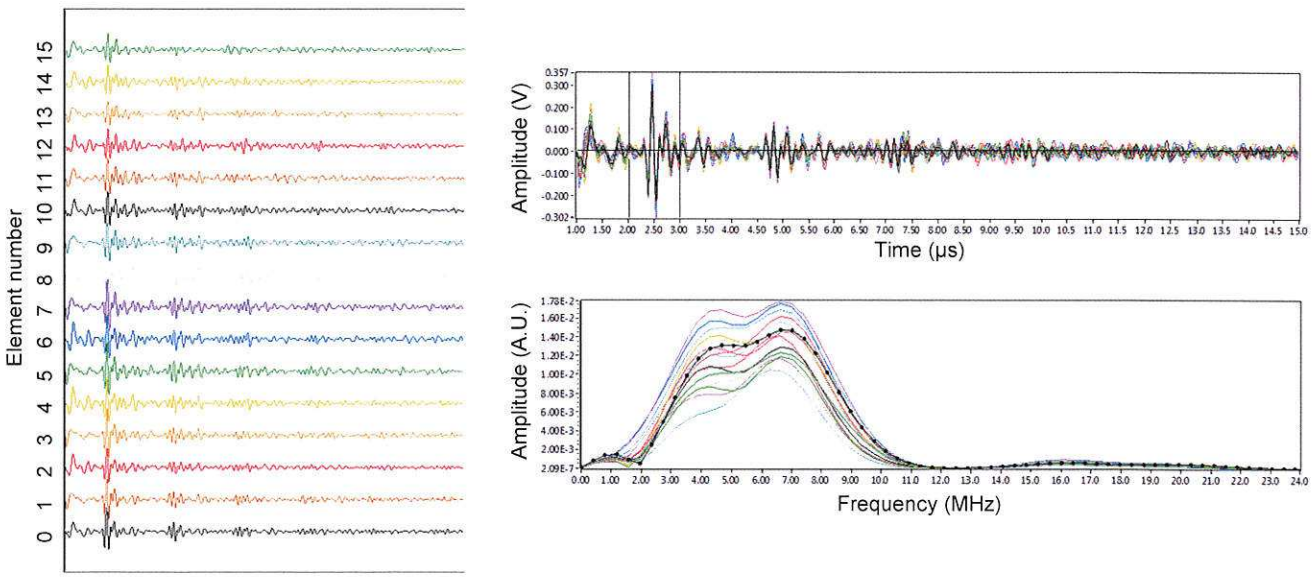

Figure 5. BIT/PZT elements time signals (pulse-echo). Top right: superimposed time signals. Bottom right: frequency spectrum of the first echo for each element.

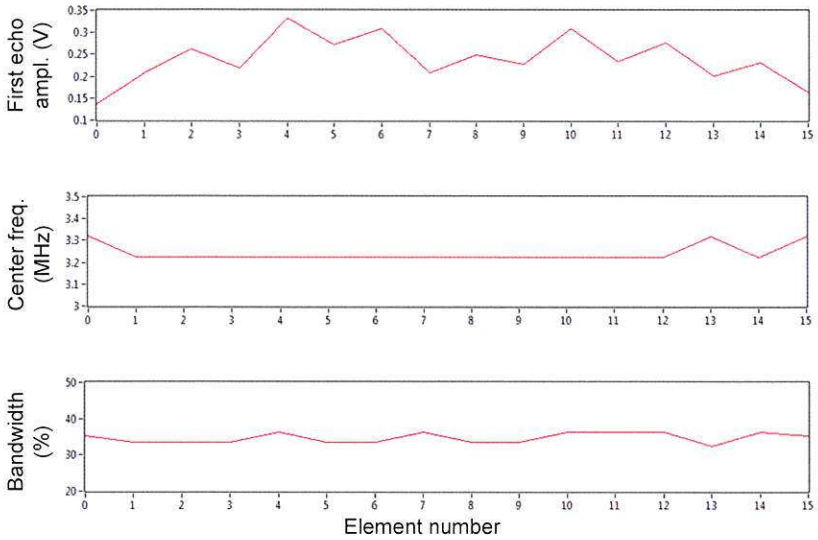

Figure 6. PZT/PZT elements first echo amplitude, frequency spectrum and -6 dB bandwidth.

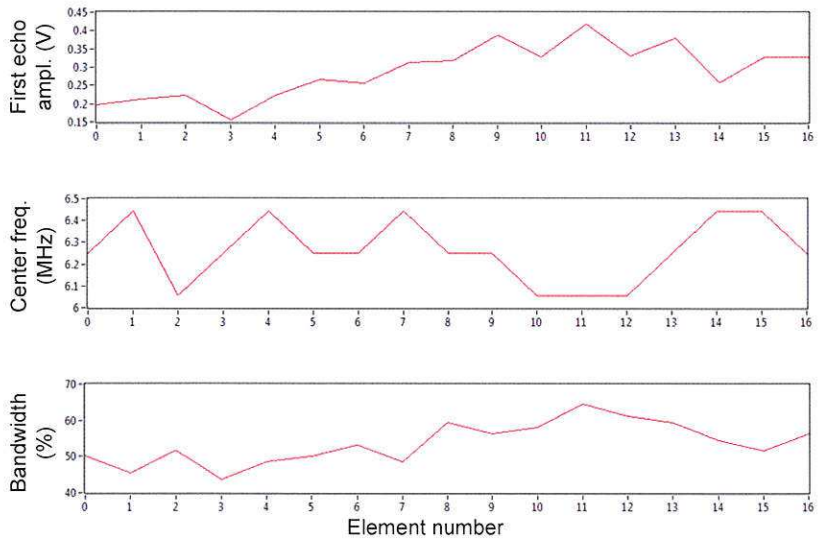

Figure 7. BIT/PZT elements first echo amplitude, frequency spectrum and -6 dB bandwidth.

4. ACOUSTIC FIELD GENERATED BY A SINGLE ELEMENT

The uniformity of the ultrasounds generated by a single IUT (one element in the array) was further assessed by the measurement of the acoustic field. This was performed using an optical probe to measure the surface displacement induced by the ultrasounds at the bottom surface of the substrate, as shown schematically in Figure 8. The PZT/PZT IUT was again driven by a Panametrics 5072PR pulser-receiver. The focal point of the optical probe was fixed in space, whereas the substrate was displaced in x and y to construct a 2D-image of the acoustic field. The step size in x and y was 1.0 mm and 1.0 mm, respectively, and the probed surface spanned an x-y region of 25 x 30 mm.

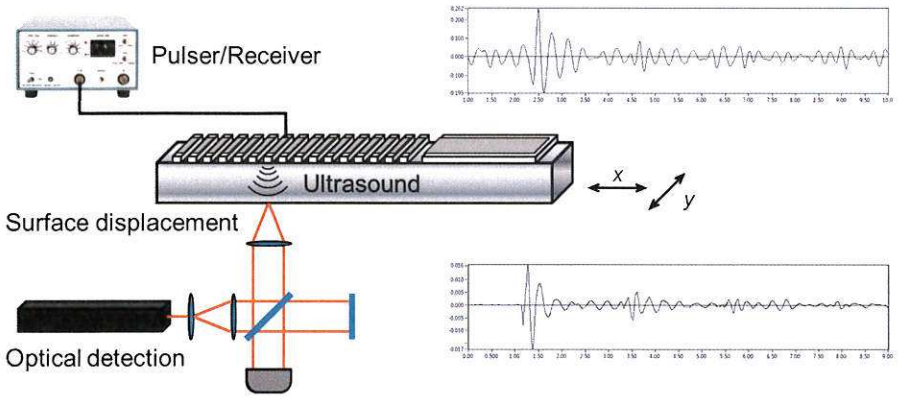

Figure 8. Schematic of the experimental setup used to measure the acoustic field generated by each element. The time signals shown on the right are obtained with the pulser-receiver (top) and the optical probe (bottom).

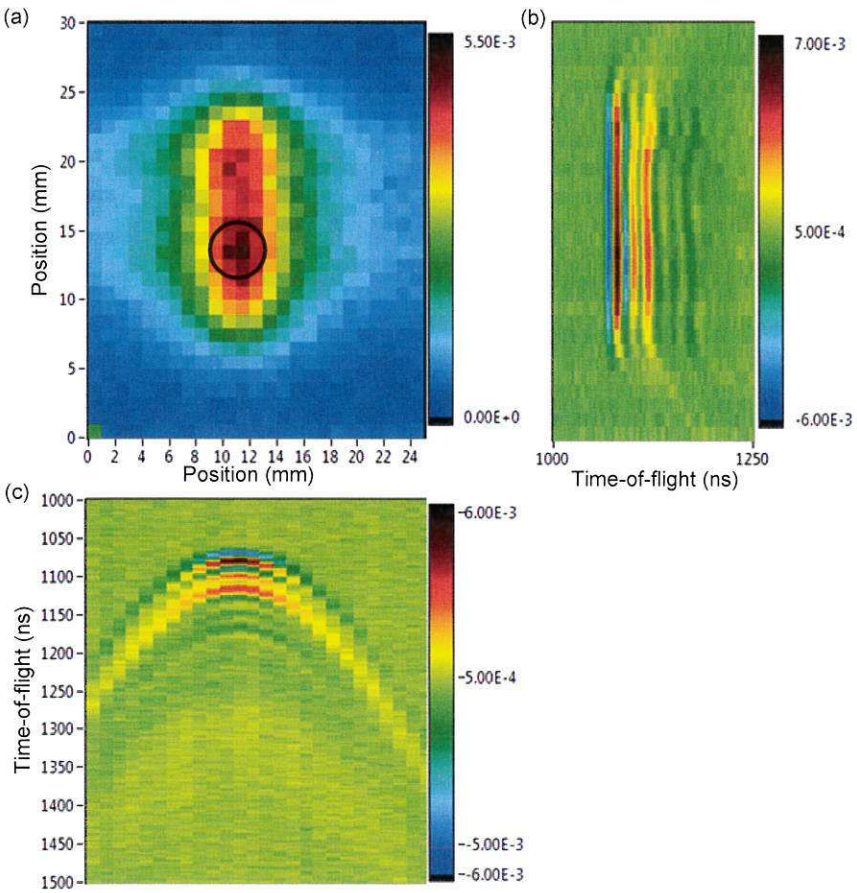

Figure 9. (a) C-scan of a typical element amplitude (rectified) generated, as detected with the optical probe. (b) B-scan of amplitude, as a function of time-of-flight and position along the length of the element. (c) Same as (b), but along the width of the element. The colorbars represent the rectified amplitude (a) and the amplitude (b) and (c).

The rectified amplitude C-scan of the element #4 is shown in Figure 9(a). Although a single IUT width corresponds to one pixel (500 μm) in the C-scan, the region of maximum amplitude roughly covers a 5 pixel-wide area, which accounts for the divergence of the ultrasound beam generated. The circled region, where the global maximum is observed, was

located directly under the point of electrical contact between the wire and the top electrode. In Figure 9(b-c), B-scans of amplitude as a function of position (ordinates in (b), abscissa in (c)) and time-of-flight (abscissa in (b), ordinates in (c)) are shown. As expected, the wavefront is flat along the length of the element (Figure 9(b)), whereas travel time is longer further from the center of the element (Figure 9(c)) to account for divergence (oblique propagation).

5. EFFECT OF TEMPERATURE

5.1 Measurement method

Since one of the main advantages of composite piezoelectric IUTs is their ability to withstand high-temperatures (shocks and cycles), the behavior of multi-elements IUTs with temperature had to be tested. This was accomplished by placing the BIT/PZT IUT array of 16 elements onto a ceramic hot plate (the back surface of the titanium alloy substrate was in direct contact with the hot plate). The temperature of the hot plate was controlled by means of a PID and the temperature at the surface of a BIT/PZT element was measured with a thermocouple. The whole setup was thermally insulated to reduce heat losses. The BIT/PZT element was driven with a Panametrics 5072PR pulser-receiver and the ultrasound signal received was recorded every minute, along with the element temperature (T), for two cycles ($T_{max} > 350°C$). The receiver gain was maintained constant over the experience.

5.2 Effect of temperature on a single element (BIT/PZT)

The results are shown in Figure 10. In (a), the time signals are illustrated for time intervals of 10 minutes during the first temperature cycle, which reached 420°C. One can appreciate the expected decrease in sound velocity with temperature by analyzing the arrival time of the first echo with respect to the dashed curve. In (b), the first echo amplitude and temperature are shown as a function of time. The signal amplitude decays rapidly with temperature in the first temperature cycle, a phenomenon attributed to the loss of piezoelectricity of the PZT matrix in the BIT/PZT composite IUT (maximum temperature reached is above the PZT Curie temperature). Then, the signal amplitude stabilizes around 0.18 V, even during the second temperature cycle. The oscillation and slight amplitude increase observed are attributed to electrical effects (the electrical contact between the wire and the top electrode was ensured solely mechanically). More reliable results, showing less variation following the initial drop, would be expected from a welded electrical connection. The experiment ended prematurely due to data acquisition issues. Still, the behavior observed for a single element IUT in the array is identical to that observed for larger IUTs studied over several months in the same laboratory: following the initial drop, the BIT/PZT IUTs signals remain fairly stable at high temperatures, with multiple cycles.

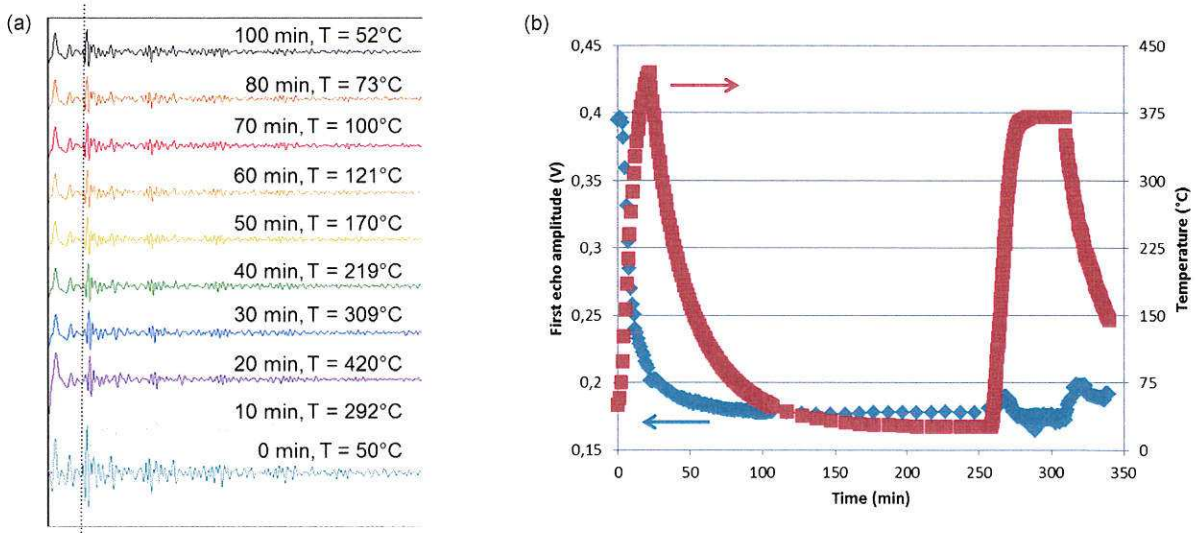

Figure 10. Effect of temperature on a single BIT/PZT element. (a) Pulse-echo signals taken at various times during the first temperature cycle. (b) First echo amplitude and temperature as a function of time, covering two temperature cycles.

6. CONCLUSIONS

Multi-element, high-temperature integrated ultrasonic transducers were fabricated from a sol-gel route. Arrays of 16 elements of PZT/PZT and BIT/PZT IUTs were machined into sol-gel sprayed / poled composite films. The elements fabricated have uniform width of 500 μm and gap of 200 μm. The amplitude of the ultrasound signals generated and detected (pulse-echo mode) by the elements of a given array are within a factor 2. This is likely due to an uneven electrical contact over/within the top electrode. Still, the center frequency and bandwidth of each element are consistent for said arrays of elements, provided the frequency response is unimodal. The acoustic field generated is also uniform over the extent of an element, as observed with an optical probe. The fabricated multi-element BIT/PZT array showed encouraging results in terms of the high-temperature resistance of its elements. Following an initial signal drop with the first temperature cycle, which is attributed to the matrix loss of piezoelectricity, the signal stabilized at half its initial magnitude. Additional temperature cycles did not adversely affect the signal amplitude.

This study has shown that multi-element arrays of PZT/PZT and BIT/PZT integrated ultrasonic transducers can be fabricated directly onto a substrate. Further work should be devoted to the improvement of the top electrode and to the incorporation of phased array approaches to the elements excitation. This shall show the aiming and focusing capabilities of the arrays of IUTs and open new field of applications for these promising devices.

REFERENCES

[1] Gandhi, M.V. and Thompson B.S., [Smart Materials and Structures], Chapman and Hall, London, (1992).

[2] Ihn J.-B. and Chang K.-K., "Ultrasonic Non-destructive Evaluation for Structure Health Monitoring: Built-in Diagnostics for Hot-spot Monitoring in Metallic and Composite Structures", in [Ultrasonic Nondestructive Evaluation Engineering and Biological Material Characterization], T. Kundu (Ed.), CRC Press, New York (2004).

[3] Wu, K.-T., Sun, Z., Kobayashi, M., Galeote, B. and Mrad, N., "Temperature Measurement in a Turbine Stator Assembly Using an Integratable High-Temperature Ultrasonic Sensor Network", Proc. SPIE 7979, Industrial and Commercial Applications of Smart Structures Technologies 2011, 797902 (April 27, 2011).

[4] Moore, P.O. (Ed.), Workman, G.L. (Ed.), Kishoni, D. (Ed.), [Nondestructive Testing Handbook, Third Edition: Volume 7, Ultrasonic Testing], ASNT (2007).

[5] Kobayashi, M., Jen, C.-K., Moisan, J.-F., Mrad, N. and Nguyen, S.B., "Integrated Ultrasonic Transducers Made by the Sol-Gel Spray Technique for Structural Health Monitoring", Smart Mater. Struct., 16(2), 317-322 (2007).

[6] Kobayashi, M., Olding, T.R., Sayer, M. and Jen, C.-K., "Piezoelectric Thick Film Ultrasonic Transducers Fabricated by a Sol–Gel Spray Technique", Ultrasonics, 39(10), 675-680 (2002).

[7] Kobayashi, M. and Jen, C.-K., "Piezoelectric Thick Bismuth Titanate/Lead Zirconate Titanate Composite Film Transducers for Smart NDE of Metals", Smart Mater. Struct., 13(4), 951-956 (2004).

[8] Kobayashi, M., Jen, C.-K., Nagata, H., Hiruma, Y., Tokutsu T. and Takenaka, T., "Integrated Ultrasonic Transducers Above 500°C", IEEE Ultrasonic Symposium, 953-956 (2007).

[9] Barrow, D.A., Petroff, T.E. and Sayer, M., "Method for Producing Thick Ceramic Films by a Sol-Gel Coating Process", United States Patent Number 5,585,136 (1996).

[10] Kobayashi, M., Jen, C.-K. and Lévesque, D., "Flexible Ultrasonic Transducers", IEEE Trans. Ultrason. Ferroelectr. Freq. Control, 53(8), 1478-1486 (2006).

[11] Dubé, N. (Ed.), [Introduction to Phased Array Ultrasonic Technology Applications: R/D Tech Guideline], Advanced Practical NDT Series, Olympus NDT, 96-161 (2004).

[12] Drinkwater, B.W. and Wilcox, P.D., "Ultrasonic Arrays for Non-Destructive Evaluation: a Review", NDT&E International, 39(7), 525-541 (2006).